THE STRUCTURE OF BARREL SHOCK IN A JET EXHAUST AT HIGH ALTITUDE

MICHIRU YASUHARA

Department of Aeronautical Engineering

(Received October 11, 1966)

1. Introduction

The inviscid flow structure of the free jets at high plenum-to-test-chamber pressure ratios can be solved by the method of characteristics although the case by case, net work integration is necessary. Owen and Thornhill[1] obtained a solution of the flow expanding into vacuum for the ratio of the specific heats of $\gamma=7/5$, and Wolff[2] obtained solutions for several values of γ. Love, Grigsby, Lee, and Woodling[3] obtained solutions for several pressure ratios, and presented the position of the jet boundary, the shape of the barrel shock, and the Mach disc, including the effect of opening angle of the nozzle at the exit. However, they did not present the variation of flow quantities between the barrel shock and the free boundary. Adamson and Nicholls[4] presented an approximate formula giving the first Mach disc shock position by assuming that the pressure just behind this shock is equal to the test chamber pressure, and also calculated the jet boundary curve applicable near the nozzle exit, and at relatively low pressure ratios with low exit flow Mach numbers. These calculations have been confirmed by several experiments[3][5][6], especially for the Mach disc position at the axial Mach number distributions. Ashkenas and Sherman[7] summarized the approximating picture of free jet expanding from a sonic nozzle, useful especially for inviscid and slightly viscous description of flow in the central core surrounded by the barrel shock and the Mach disc, and gave some concise and easily-employed approximate formulae applicable in high supersonic regions.

These studies show that at high pressure ratios, the flow property in the isentropic core looks very similar to the source flow, and for example, the density ρ is proportional to the inverse square of radial distance r from the imaginary source, although there is some angular dependency. For the sonic nozzle flow, Sherman and Ashkenas proposed that $\rho r^2 \propto \cos^2\frac{\pi\bar{\theta}}{2\Phi}$ where $\bar{\theta}$ is the polar angle measured from the nozzle axis, and Φ is a function of the ratio of the specific heats, γ. This angular dependency looks especially to be a result of the interaction between the expansion waves emanating from the edge of the nozzle exit, and it will be possible to eliminate this effect by taking some care in designing the exit nozzle, for a given pressure ratio. In the preceding paper[12], the author treated the flow field in the barrel shock layer theoretically, and presented a set of similarity equations under the assumption of hypersonic pure source flow. In the present paper, the numerical results of the practical calculation will be presented.

2. Source Flow and Barrel Shock

Consider an inviscid, uniform, steady source flow with total spreading angle of $2\theta_0$, expanding cylindrically or spherically into vacuum. It is assumed that the flow is uniformly expanded, and the every flow quantity is a function of radial distance r from the source, alone. If each quantity is referred to the

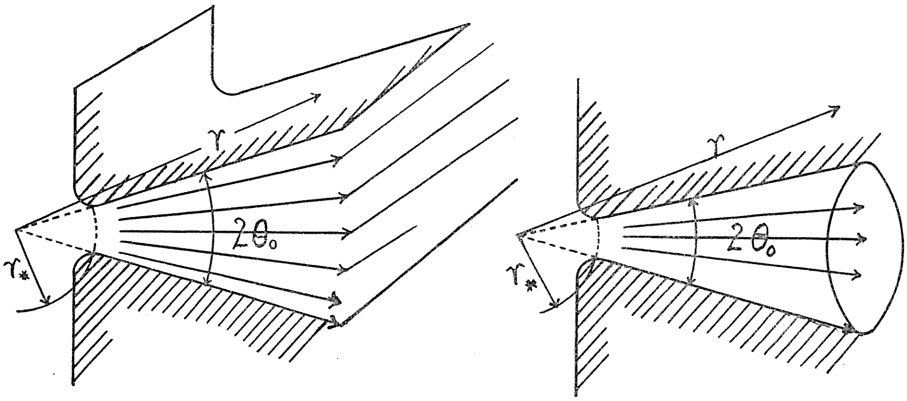

(a) Cylindrical Case (b) Spherical Case

FIG. 1. Source Flow Expanding into Vacuum.

sonic condition, denoted by the subscript "*", then for sufficiently high Mach numbers:

$$\left(\frac{r_*}{r}\right)^\beta=\frac{M}{\left\{\frac{2}{\gamma+1}+\frac{\gamma-1}{\gamma+1}M^2\right\}^{(\gamma+1)/2(\gamma-1)}}\doteqdot\left(\frac{\gamma+1}{\gamma-1}\right)^{(\gamma+1)/2(\gamma-1)}M^{-2/(\gamma-1)}, \tag{1}$$

$$\frac{T}{T_*}=\frac{1}{\frac{2}{\gamma+1}+\frac{\gamma-1}{\gamma+1}M^2}\doteqdot\frac{\gamma+1}{\gamma-1}M^{-2}, \tag{2}$$

$$\frac{p}{p_*}=\left(\frac{T}{T_*}\right)^{\gamma/(\gamma-1)}\doteqdot\left(\frac{\gamma+1}{\gamma-1}\right)^{\gamma/(\gamma-1)}M^{-2\gamma/(\gamma-1)}, \tag{3}$$

$$\frac{\rho}{\rho_*}=\left(\frac{T}{T_*}\right)^{1/(\gamma-1)}\doteqdot\left(\frac{\gamma+1}{\gamma-1}\right)^{1/(\gamma-1)}M^{-2/(\gamma-1)}, \tag{4}$$

$$\frac{u}{u_*}=M\left(\frac{T}{T_*}\right)^{1/2}\doteqdot\left(\frac{\gamma+1}{\gamma-1}\right)^{1/2}, \tag{5}$$

where M, T, p, ρ, and u denote the Mach number, the temperature, the pressure, the density, and the radial velocity of the flow at r, and γ is the ratio of specific heats, respectively. Also, β equals to unity in a cylindrical case, and two in a spherical case. From these relations, it is easily seen that the pressure is a decreasing function of r. These relations are applicable for $M\geq 1$.

To keep the spreading angle constant, it is necessary to put a wall outside the flow region (or to apply a distributed pressure along the boundary stream lines to balance with the ones on these lines, which is not practical).

Now remove the wall beyond $r=r_A$ where the pressure $p(r_A)$ is p_∞, and, instead of the wall, apply a constant pressure p_∞ in the wall-removed vacant region. Then, because the pressure of the source flow at r, larger than r_A, is smaller than p_∞, the flow boundary is pushed inward which results in the formation of a higher pressure and higher density region outside the source flow, and thus the shock wave is formed as the boundary of the two regions, as shown in Fig. 2.

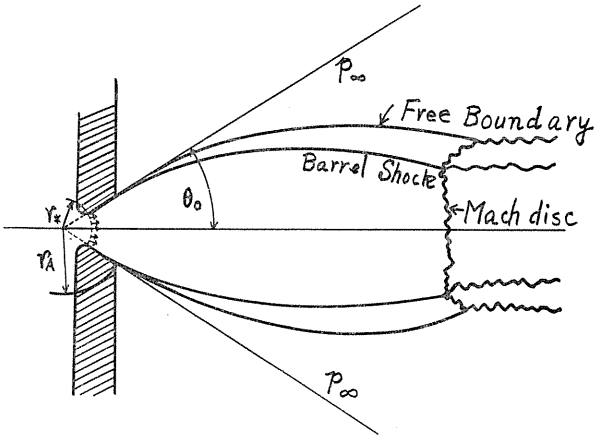

FIG. 2. Formation of Barrel Shock.

This gives a simplified picture of the barrel shock in the free jets at high plenum-to-test-chamber pressure ratios. In some cases, the gas pressure p_e at the nozzle exit is still higher than the test chamber pressure p_∞, and there is further expansion accompanied by the expansion waves at the nozzle exit, and these waves give deviations from the ideal source flow in the downstream.

The flow of this type continues down to a Mach disc shock behind which the pressure is of the order of p_∞. The present paper treats the flow between the barrel shock and the free boundary, from the standpoint of the hypersonic flow theory, and the pure source type flow is assumed in the isentropic core. The effects of the deviation from the pure source flow is not discussed.

3. Newton-Busemann Approximation to the Barrel Shock.

First, it is useful to observe the Newtonian approximation in order to see some fundamental features of the hypersonic barrel shocks. In the limiting case of $\gamma \to 1$ and $M \to \infty$, the shock relation gives the pressure p_s just behind the shock as follows :

$$p_s = \rho_1 u_1^2 \sin^2 \sigma, \tag{6}$$

where the subscripts "1" and "s" denote quantities just ahead of and behind the shock wave, and σ is the angle between the shock and the radial line. This is known as the Newtonian relation when p_s is identified to the pressure along the flow boundary or a body surface. Busemann[8] made a correction to the above relation due to the centrifugal force effect. This is followed in the present case using the polar coordinates. In Fig. 3, actually the thickness of the shock layer

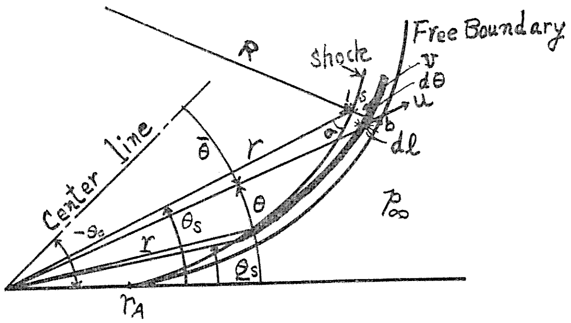

FIG. 3. Newton-Busemann Description of Barrel Shock.

is infinitesimally small, because in the Newtonian limit, γ tends to unity. Let the shock position be denoted by $\theta_s=\theta_s(r)$. At this position, the pressure difference dp_c in the infinitesimal layer composed of particles which collided with the surface near $\underline{\theta}_s$ and which have the velocity $U(\underline{\theta}_s)$ is[9]:

$$dp_c=\frac{\rho(\theta_s,\underline{\theta}_s)U^2(\underline{\theta}_s)}{R(\theta_s)}dl,$$

where dl is the thickness of this layer, and R the radius of curvature of this stream tube which is almost the same as the curvature of both the shock wave and the free boundary. From the conservation of mass:

$$\rho(\theta_s,\underline{\theta}_s)U(\underline{\theta}_s)\{2\pi r\sin(\theta_0+\theta_s)\}^{\beta-1}dl$$
$$=\rho_1(\underline{\theta}_s)u_1(\underline{\theta}_s)\{2\pi\underline{r}\sin(\theta_0+\underline{\theta}_s)\}^{\beta-1}\underline{r}d\underline{\theta}_s,$$

and also from the relations:

$$\frac{1}{R}=\frac{\sin\sigma}{r}\Big(\frac{d\sigma}{d\theta_s}+1\Big),\qquad U(\underline{\theta}_s)=u_1(\underline{\theta}_s)\cos\underline{\sigma},$$

$$\rho_1u_1^2\fallingdotseq\Big(\frac{\gamma+1}{\gamma-1}\Big)^{1/2}\rho_*u_*^2(r_*/r)^\beta,\ (M_1\gg1)$$

the total pressure difference between the shock wave and the free boundary is integrated to give:

$$p_c=\Big(\frac{\gamma+1}{\gamma-1}\Big)^{1/2}\rho_*u_*^2r_*^\beta\frac{\sin\sigma\Big(\dfrac{d\sigma}{d\theta_s}+1\Big)}{r^\beta\sin^{\beta-1}(\theta_0+\theta_s)}\int_0^{\theta_s}\cos\underline{\sigma}\sin^{\beta-1}(\theta_0+\underline{\theta}_s)d\underline{\theta}_s,$$

and thus, the pressure on the flow boundary is:

$$p_b=p_s+p_c=\Big(\frac{\gamma+1}{\gamma-1}\Big)^{1/2}\rho_*u_*^2r_*^\beta$$
$$\times\Big[\frac{\sin^2\sigma}{r^\beta}+\frac{\sin\sigma\Big(\dfrac{d\sigma}{d\theta_s}+1\Big)}{r^\beta\sin^{\beta-1}(\theta_0+\theta_s)}\int_0^{\theta_s}\cos\underline{\sigma}\sin^{\beta-1}(\theta_0+\underline{\theta}_s)d\underline{\theta}_s\Big],\qquad(8)$$

where
$$\tan\sigma = \frac{rd\theta_s}{dr} \tag{9}$$

Eqs. (8) and (9) with the boundary conditions that:

$$\theta_s = 0 \qquad \text{at} \qquad r = r_A, \tag{10}$$

will give the solution $\theta_s=\theta_s(r)$ for a given free stream pressure $p_b=p_\infty$. It is rather tedious to solve Eq. (8), and therefore, as a first approach, Eq. (6), neglecting the centrifugal force, is solved as follows. By putting $p_s=p_\infty$, Eq. (6) is re-written as:

$$n \equiv \frac{p_\infty}{\rho_* u_*^2}\left(\frac{\gamma-1}{\gamma+1}\right)^{1/2} = \left(\frac{r_*}{r}\right)^{\beta}\frac{r^2\theta_s'^2}{1+r^2\theta_s'^2}.$$

This is solved in closed forms, giving:

$$\begin{aligned} &\beta=1: \qquad \theta_s = 2\left\{\sin^{-1}\sqrt{n\frac{r}{r_*}} - \sin^{-1}\sqrt{n\frac{r_A}{r_*}}\right\}, \qquad \left(n\frac{r}{r_*}\leq 1,\right) \\ &\beta=2: \qquad \theta_s = \sin^{-1}\sqrt{n}\frac{r}{r_*} - \sin^{-1}\sqrt{n}\frac{r_A}{r_*}, \qquad \left(\sqrt{n}\frac{r}{r_*}\leq 1,\right) \end{aligned} \tag{11}$$

where :

$$n = \frac{1}{\gamma}\left(\frac{\gamma-1}{\gamma+1}\right)^{(\gamma+1)/2}\left(\frac{r_*}{r_A}\right)^{\beta\gamma}, \quad \frac{r_A}{r_*} = \left(\frac{\gamma-1}{\gamma+1}\right)^{1/2\beta}\left(\frac{p_*}{p_0}\,\frac{p_0}{p_\infty}\right)^{1/\beta\gamma}. \tag{12}$$

As another approach, let the centrifugal force effect be retained, but it is assumed that:

$$\tan\theta_0 \gg \theta_s, \quad 1 \gg \theta_s. \tag{13}$$

In this case, after terms of order θ_s^2 is neglected compared to unity, Eq. (8) is reduced to :

$$n = \left(\frac{r_*}{r}\right)^{\beta}\left[r^2\theta_s'^2 + r\theta_s(2\,\theta_s' + r\theta_s'')\left\{\frac{\sin\theta_0 + \frac{\theta_s}{2}\cos\theta_0}{\sin\theta_0 + \theta_s\cos\theta_0}\right\}^{\beta-1}\right]. \tag{14}$$

In the above equation, if the last factor of the right-hand side is approximated by unity for $\beta=2$, then Eq. (14) can be integrated to give:

$$\begin{aligned} \theta_{s_0}^2 &= \frac{2n}{(1+\beta)}\left[\frac{1}{\beta}\left\{\left(\frac{r}{r_*}\right)^{\beta} - \left(\frac{r_A}{r_*}\right)^{\beta}\right\} - \left(\frac{r_A}{r^*}\right)^{\beta}\left(1-\frac{r_A}{r}\right)\right] \\ &= \frac{2n}{\beta(1+\beta)}\left(\frac{r_A}{r_*}\right)^{\beta}\left[\left(\frac{r}{r_A}\right)^{\beta} - 1 - \beta\left(1-\frac{r^A}{r}\right)\right]. \end{aligned} \tag{15}$$

Eq. (15) is indicative in understanding the barrel shock shape of the present model. If $r \gg r_A$, the leading term gives that $\theta_{s_0} \fallingdotseq \sqrt{\frac{2n}{\beta(\beta+1)}}\left(\frac{r}{r_*}\right)^{\beta/2}$, and this suggest that the similarity treatment for $\gamma \neq 1$ will be possible in analysing the flow. More accurate solution of Eq. (8) or (14) can be obtained by the sucessive approximation starting from Eq. (15).

Two things must be noted in comparing the present calculations with experiments. First, in usual hypersonic flows passing a convex body, the solution with the centrifugal force effects may not give a better comparison with the accurate solution than that without the centrifugal force effects, and inversely, for a concave body, the solutions may give a better results. In the present problem, the flow geometry is similar to the flow passing the concave body, and therefore the centrifugal force correction is expected to give a better comparison with the accurate solutions. Second, for the free jet expanding from a circular sonic nozzle, Ashkenas and Sherman[7] proposed an approximate formula for the density field in the isentropic core, such that ρr^2 is a function of $\bar{\theta}$, which means that the isentropic core is not of a source-type flow but a source-like one, which is not discussed in the present paper.

Figs. 4 a and 4 b show barrel shock shapes calculated by Eq. (11) and Eq. (15) for $p_0/p_\infty=100$ and 36.7, respectively, where the value of γ has been taken to be 7/5 in calculating the flow in the isentropic core.

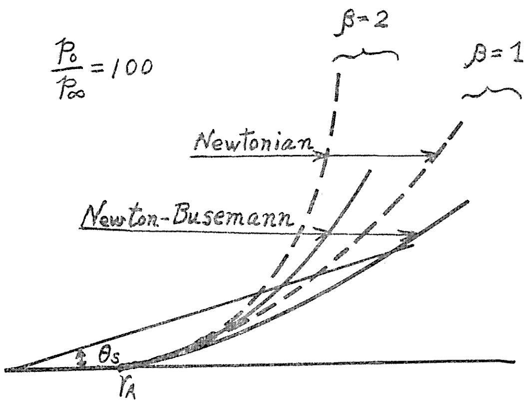

FIG. 4 a. Barrel Shock of the Spherical Flow ($\beta=2$) and the Cylindrical Flow ($\beta=1$).

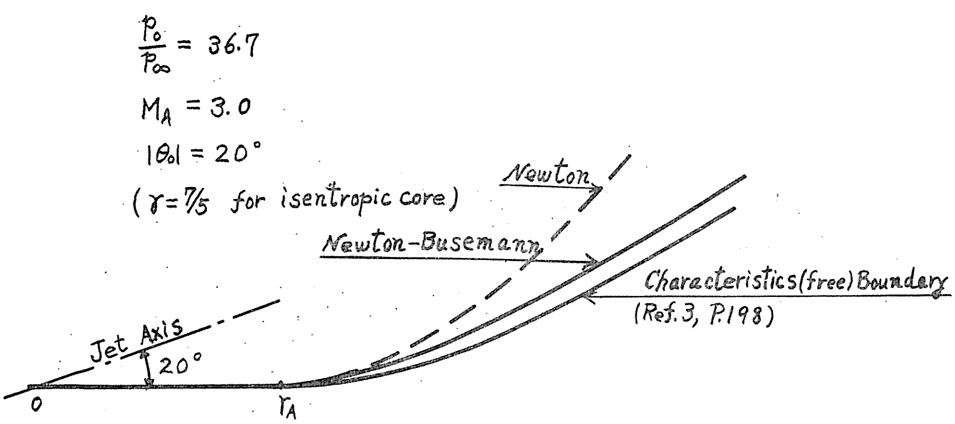

FIG. 4 b. Barrel Shock of the Spherical Flow Compared with the Free Boundary Calculated by the Characteristic Method.

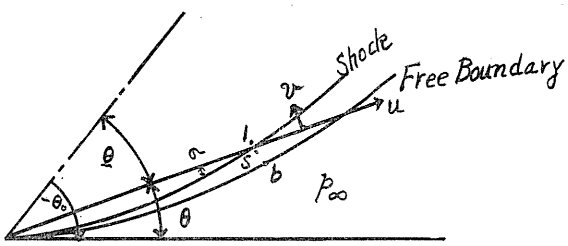

FIG. 5. Coordinates System Chosen for Shock Layer Calculation.

4. Similarity Calculation

Under the assumption of pure source flow with spreading angle of $2\theta_0$, the hypersonic small disturbance theory can be applied to the present barrel shock flow, which is given in ref. (12) by the present author, and it was found that there are similarity solutions within the hypersonic small disturbance theory. The numerical solutions of Eqs. (9) of ref. (12) are obtained for $n=\beta/2$ where $\beta=1$ or 2, $\gamma=7/5$ or $5/3$, respectively. Integrations are made by starting from $\eta=1$ toward $\eta=\eta_b$ where $\eta_b=\overline{V}_{0b}$, which is smaller than unity. At the free boundary, the solutions have singularity, that is, the density goes up to infinity, and therefore near this boundary, power reprentations of solution are matched with the numerical solution at some value of η close to η_b. Some of the calculated values are tabulated as follows:

β	γ	η_b	$\overline{V}_{0b}$	P_{0b}
1	5/3	0.940	0.940	2.91
	7/5	0.962	0.962	3.08
2	5/3	0.936	0.936	2.43
	7/5	0.959	0.959	2.30

where the quantities at the free boundary, denoted by the subscript "b" are expressed as follows:

$$\eta_b=\frac{\theta_b}{\theta_s},\quad p_b=p_*\gamma\left(\frac{\gamma+1}{\gamma-1}\right)^{1/2}\left(\frac{r_*}{r}\right)^{\beta}(r\theta_s')^2P_{0b},$$

$$\rho_b=\rho_*\left(\frac{\gamma-1}{\gamma+1}\right)^{1/2}\left(\frac{r_*}{r}\right)^{\beta}R_{0b},\quad v_b=u_*\left(\frac{\gamma+1}{\gamma-1}\right)^{1/2}(r\theta_s')\overline{V}_{0b},\tag{16}$$

$$\theta_b=\delta\left(\frac{r}{r_*}\right)^{\beta/2}=\eta_b\theta_s,$$

where:

$$\delta=\frac{2}{\beta}\sqrt{\frac{n}{\gamma P_{0b}}}\left(\frac{\gamma-1}{\gamma+1}\right)^{1/4}.$$

Also numerical solutions are plotted in Fig. 6. The figures show that the pressure and the angular velocity do not change appreciably from the shock to the free boundary, whereas the density goes up to infinity at the free boundary, which

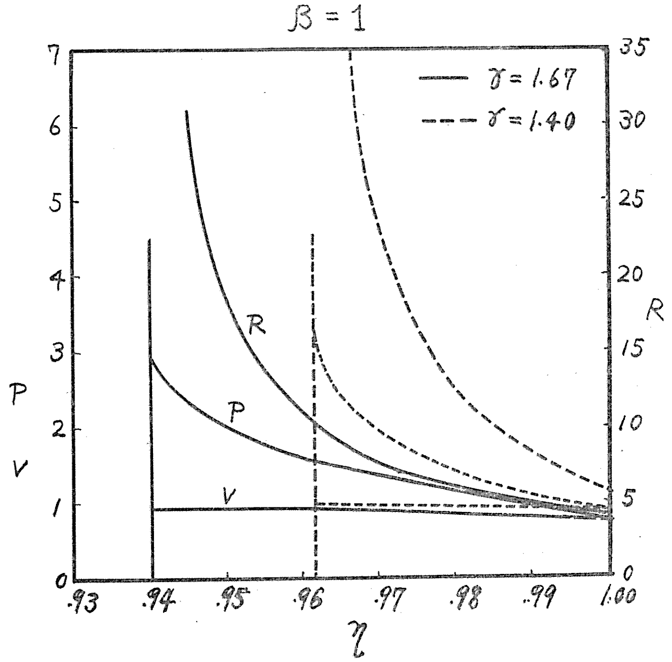

FIG. 6 a. Shock Layer Solution for Cylindrical Case ($\beta=1$).

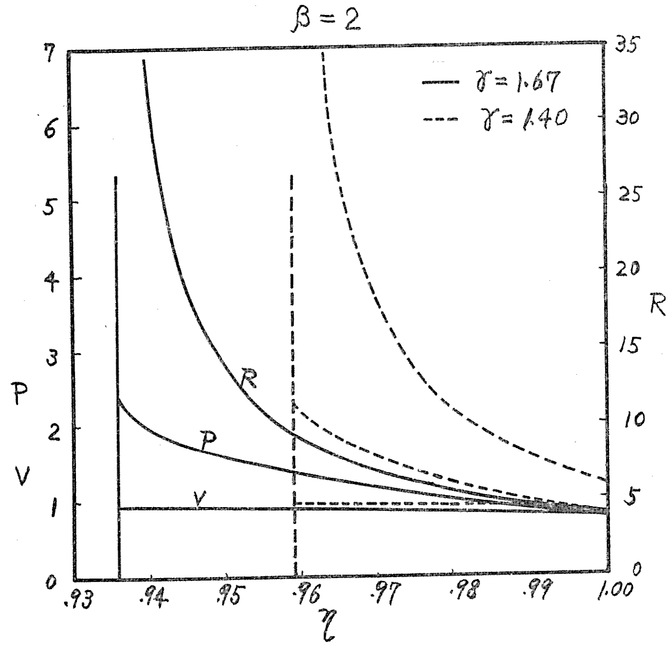

FIG. 6 b. Shock Layer Solution for Spherical Case ($\beta=2$).

means that the gas temperature goes down to zero at the free boundary in the equilibrium, perfect gas flows.

It must be added some arguments about the shock position. Eq. (16) shows that $\theta_S=0$ at $r=0$, and θ_S is a monotonically increasing function of r. However, the pure source flow can not exist for the value of r smaller than r_*, corresponding to the sonic point, and also in the present theory it is assumed that, in the source flow region, the Mach number M is much larger than unity. This is not correct near the sonic point r_*, and therefore in the theory, r/r_* must be much larger than unity. Also, as shown in Fig. 2, the shock starts from r_A, where actually the shock is a Mach line, and therefore the initial condition on the shock shape must be $\theta_S=0$ at $r=r_A$, which is not satisfied by Eq. (16) except when quantities of order (r_A/r) is neglected. Thus, similarity solution should be accepted under the condition; $r_A/r \ll 1$.

The similarity solutions give the same leading terms as the Newton-Buseman approximation Eq. (15), except the proportionality constants. To obtain higher order approximations, three kinds of terms should be taken into account, that is; $0(r_A/r)$, $0(1/M_1^2\sigma^2)$, and $0(\theta/\theta_0)$, which can be accomplished by the similar method as Kubota's[11] series expansion.

The range of applicability of the similarity solution is given in ref. (12), or more precisely, by:

$\beta=1$:

$$(\gamma+1)^{-(\gamma+1)/2(\gamma-1)}(\gamma-1)^{-1/2},\ \left(\frac{p_\infty}{p_*}\right)^{-1/\gamma}\left(\frac{\gamma-1}{\gamma+1}\right)^{1/2} \ll r/r_* \ll \left(\frac{p_\infty}{p_*}\right)^{-1}\left(\frac{\gamma+1}{\gamma-1}\right)^{1/2},$$

$\beta=2$: (17)

$$(\gamma+1)^{-(\gamma+1)/4(\gamma-1)}(\gamma-1)^{-1/4},\ \left(\frac{p_\infty}{p_*}\right)^{-1/2\gamma}\left(\frac{\gamma-1}{\gamma+1}\right)^{1/4} \ll r/r_* \ll \left(\frac{p_\infty}{p_*}\right)^{-1/2}\tan\theta_0\left(\frac{\gamma+1}{\gamma-1}\right)^{1/4},$$

$\beta=1,\ 2$:

$$r_A/r \ll 1.$$

In addition to the above limitation, the effect of expansion waves or compression waves at the nozzle exit, if any, or real gas effects such as viscosity, heat conductivity and further rarefied gas effects should be accounted for.

Conclusion

The cylindrical or spherical source flow with a finite initial spreading angle and with a constant free boundary pressure, is analysed from the standpoint of the inviscid, hyperonic flow theory. First, Newton-Busemann approximation is used to see the fundamental behaviour of the barrel shock shape, and it is found that the angular shock position $\theta_S(r)$ measured from the initial free boundary, is proportional to $r^{\beta/2}$ for a large value of $r(\gg r_A)$, where $\beta=1$ for cylindrical case and $\beta=2$ for spherical case. Second, the numerical calculations of the hypersonic small disturbance equations, derived in ref. (12), are made and plotted in Figs. 6 to see the change of flow quantities in the shock layer. Last, the angular dependency of flow quantities in the isentropic core, caused by the expansion waves at the nozzle exit, is not discussed.

References

1) P. L. Owen, and C. K. Thornhill, The Flow in an Axially Symmetric Supersonic Jet From a Nearly Sonic Orifice into Vacuum, ARC, R and M 2616 (1948).
2) F. S. Sherman, Self Similar Development of Inviscid Hypersonic Free Jet Flows, Lockheed Rep. 6-90-63-61 (1963).
3) E. S. Love, C. E. Grigsby, L. P. Lee and M. J. Woodling, Experimental and Theoretical Studies of Axisymmetric Free Jets, NASA TR R-6 (1959).
4) T. C. Adamson, Jr. and J. A. Nicholls, On the Structure of Jets From Highly Underexpanded Nozzles into Still Air, J. Aerospace Sci., **26**, 16 (1959).
5) K. Bier, and B. Schmidt, Zur Form der Verdichtungsstossen in frei expandierenden Gasstrahlen, Z. Angew. Phys., **13**, 493 (1961).
6) V. H. Reis and J. B. Fenn, Separation of Gas Mixtures in Supersonic Jets, J. Chem. Phys., **39**, 3240 (1963).
7) H. Ashkenas and F. S. Sherman, The Structure and Utilization of the Supersonic Free Jets in Low Density Wind Tunnels, in "Rarefied Gas Dynamics", ed. by DeLeeuw, J. H., Academic Press, **Vol. II** (1965).
8) A. Busemann, Fluessigkeits-und-Gasbewegung, Handwoerterbuch der Naturwissenschaften, Bd. IV, Gustav Fischer, Jena, 244-279 (1933).
9) G. G. Cherni, Introduction to Hypersonic Flow, Academic Press, 122 (1961).
10) H. W. Emmons ed., Fundamentals of Gas Dynamics, Princeton University Press, 57 (1958).
11) T. Kubota, Inviscid Hypersonic Flow over Blunt-Nosed Slender Bodies, GALCIT Publications No. 417 (1957).
12) M. Yasuhara, Hypersonic Self-Similarity of Barrel Shock in Source Type Free Jets, AIAA, **4**, 6, (1966).